JOURNAL OF CHEMICAL INFORMATION AND MODELING

Article

pubs.acs.org/jcim

Interactions between Voltage Sensor and Pore Domains in a hERG K^+ Channel Model from Molecular Simulations and the Effects of a Voltage Sensor Mutation

Charlotte K. Colenso,[†] Richard B. Sessions,[†] Yi H. Zhang,[‡] Jules C. Hancox,[‡] and Christopher E. Dempsey*[,†]

[†]School of Biochemistry, Medical Sciences Building, University of Bristol, University Walk, Bristol BS8 1TD, U.K.

[‡]School of Physiology and Pharmacology and Cardiovascular Research Laboratories, Medical Sciences Building, University of Bristol, University Walk, Bristol BS8 1TD, U.K.

Supporting Information

ABSTRACT: The hERG K^+ channel is important for establishing normal electrical activity in the human heart. The channel's unique gating response to membrane potential changes indicates specific interactions between voltage sensor and pore domains that are poorly understood. In the absence of a crystal structure we constructed a homology model of the full hERG membrane domain and performed 0.5 μs molecular dynamics (MD) simulations in a hydrated membrane. The simulations identify potential interactions involving residues at the extracellular surface of S1 in the voltage sensor and at the N-terminal end of the pore helix in the hERG model. In addition, a diffuse interface involving hydrophobic residues on S4 (voltage sensor) and pore domain S5 of an adjacent subunit was stable during 0.5 μs of simulation. To assess the ability of the model to give insight into the effects of channel mutation we simulated a hERG mutant that contains a Leu to Pro substitution in the voltage sensor S4 helical segment (hERG L532P). Consistent with the retention of gated K^+ conductance, the L532P mutation was accommodated in the S4 helix with little disruption of helical structure. The mutation reduced the extent of interaction across the S4−S5 interface, suggesting a structural basis for the greatly enhanced deactivation rate in hERG L532P. The study indicates that pairwise comparison of wild-type and mutated channel models is a useful approach to interpreting functional data where uncertainty in model structures exist.

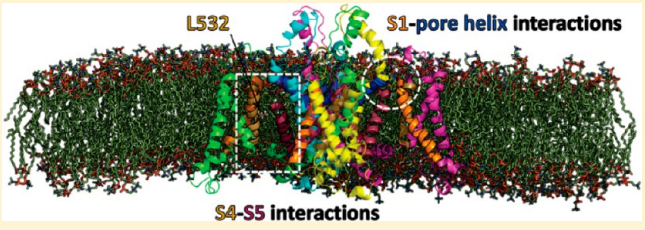

INTRODUCTION

The generation and propagation of electrical signals in excitable tissues is mediated by voltage-sensitive Na^+, Ca^{2+}, and K^+ channels that undergo gating transitions in response to changes in the membrane potential. Many voltage-gated K^+ channels have been identified and functionally characterized, and in several key examples high-resolution crystal structures have been determined (e.g., refs 1−4), facilitating understanding of the complex functional properties of these channels. Of particular interest are questions about the mechanisms of transmission of membrane potential changes to channel gating mediated by K^+ channel voltage sensor domains, and the structural basis for channel inactivation. Since these are dynamic processes involving large-scale conformational changes within and between subunits, detailed understanding will require structural and functional analyses that define different states within gating pathways, and the use of molecular dynamics (MD) simulations to characterize the nature of transitions between these states. Considerable progress is being made in these areas (e.g., refs 5−8).

The application of MD simulation to K^+ channels that lack crystal structures is challenging since the starting structure must necessarily be a model constructed using sequence homologies with crystallized channel proteins, and possibly refined using low-resolution structural information (e.g., residue accessibility studies and the effects of residue-specific mutagenesis). However, MD simulations of homology models have considerable potential in several respects. The stability of the model during simulation may give insight into the extent to which the model (or parts of the model) is faithfully constructed in the starting structure.[9] Identification of stable inter-residue or interdomain interactions can provide a context for experimental mutagenesis studies to assess the presence of these interactions and their functions in the real protein. As the ability to run multinanosecond to microsecond MD simulations advances with extended computational power and improved parametrization of united-atom and coarse-grained methods,[10] complementary rounds of experimental analyses and model refinement may allow an iterative approach to model improvement. Finally, MD simulation of channel mutant models is likely to be helpful in interpreting the functional effects of mutations in structural terms.

Received: January 30, 2013
Published: May 14, 2013

The hERG potassium channel (human Ether-à-go-go-Related Gene; alternative nomenclature KCNH2 or Kv11.1) is a key example where the absence of a crystal structure has limited detailed understanding of the unique functional properties of this protein. The hERG channel carries the rapid, delayed rectifier repolarizing current (I_{Kr}) that controls the duration of the QT interval of the human ventricular action potential.[11] This function is mediated by a rapid channel inactivation following channel opening at depolarized membrane potentials, followed by a rapid recovery from inactivation and slow channel closing on repolarization (Figure S1 in Supporting Information [SI]).[11] These properties indicate a unique interplay between voltage-sensing and pore domain subunits in hERG that is incompletely understood. Additionally, hERG is sensitive to pharmacological inhibition by a variety of drugs, and this has promoted efforts to define drug binding determinants from the effects on channel block of hERG mutants in alanine-scanning studies, supplemented with computational docking to homology models constructed on pore domain crystal structures.[12−18] These studies parallel concerted efforts to redesign pharmacologically useful drugs that eliminate problematic issues associated with adventitious hERG channel block.[19]

Although several pore domain homology models of hERG have been made to study drug block[12−18] and to probe mechanisms of C-type inactivation,[20,21] computational studies involving the full membrane domain comprising both voltage sensor and pore elements have been limited.[22,23] In this study we describe the construction of a homology model of the full membrane domain of hERG built onto the crystal structure template of the Kv1.2/2.1 chimera structure,[3] its incorporation within a hydrated POPC membrane patch and 0.5 μs MD simulation at 37 °C. This simulation was performed to assess the nature of interactions between voltage-sensing and pore domains in the open state. Of particular interest is evidence that interactions between the voltage sensor and pore helix of voltage-sensitive K^+ channels may "anchor" less-mobile elements of the voltage sensor domain, increasing the efficiency of the voltage sensor−pore coupling as mobile elements of the voltage sensor domain move in response to changes in membrane potential.[24] We also characterize the nature of direct interactions between S4 (voltage sensor domain) and S5 (pore domain) in our model in the light of functional data in the literature on mutations at the potential S4−S5 interface.

To explore the potential of the model to give insight into the functional consequences of channel mutants we have also run an equivalent simulation of a hERG channel model with a leucine to proline mutation in the S4 helix of the voltage sensor (hERG L532P). We chose this mutant since the introduction of a proline into a helical element is potentially structurally disruptive[25] and thus likely to have effects on local structure that may be assessed by MD. This mutant was recently constructed experimentally in the study of the accelerated repolarization disorder short QT syndrome, since reggae mutant zebrafish with the homologous mutation (zERG L499P) display arrhythmias associated with shortening of the QT interval.[26] Importantly, the hERG L532P channel is functional and retains voltage-dependent gating.[26,27] However, the channel displays accelerated activation and particularly rapid closing (deactivation) kinetics (Figure S1 in SI), indicating perturbation of the coupling between voltage sensor and pore domains. A comparison of the MD simulations of the wild-type and hERG L532P models supports the conclusion that direct interactions between S4 and S5 in hERG may modulate the gating properties of the channel and that perturbation of these interactions contributes to altered gating kinetics in hERG L532P.

METHODS

Homology Modeling. Homology models of open-state wild-type and L532P mutant hERG channels were constructed based on the crystal structure of a Kv1.2/2.1 "paddle chimera" (PDB: 2R9R).[3] The sequence alignment was initially performed using ClustalW2[28,29] and TMPred[30] and was subsequently refined using published structural and functional data as described in the Results. The transmembrane helical residues of hERG were aligned using information on conserved residues[3,24,31−33] and were mutated manually within InsightII (Accelrys; San Diego, CA, U.S.A.). Linker regions including the S5−P linker (turret) were found using the Search Loop function within InsightII. The wild-type hERG model was modified with a single-residue substitution to produce the L532P mutant. Tetrameric models were constructed by superimposing hERG monomers onto the Kv1.2/2.1 tetramer. The template crystal structure contains four bound ions (K^+) (1) in the selectivity filter, two of which were substituted with water molecules (0) to yield a 0101 filter occupancy state as counted from the extracellular side, in accordance with previous simulations using the KcsA channel.[34] Steric clashes between side chains were resolved by adjusting the rotameric state of the residues involved. hERG models were subjected to a total of 1800 iterations of steepest descent and conjugate gradient energy minimization using Discover, and were evaluated using PROCHECK.[35] Since the models comprise only the membrane domain of hERG, the N- and C-terminal residues are not the true termini of the hERG channel and were left uncharged.

Molecular Dynamics Simulations. Molecular dynamics simulations of wild-type and L532P mutant hERG channels embedded within a 1-palmitoyl-2-oleoyl-*sn*-glycero-3-phosphocholine (POPC) bilayer were performed using GROMACS 4.5.3.[36] An equilibrated bilayer containing 64 POPC lipids in each bilayer leaflet was downloaded from the Tieleman Web site[37] and replicated in the x and y dimensions to yield a 3 × 3 × 1 lipid box. The simulation box was resized to 20 nm × 20 nm × 14(z) nm and solvated with a 15 Å layer of water in the $\pm z$ dimension to account for periodicity. The lipid−solvent system was energy minimized with the steepest descent method for 1000 steps and subject to a 5-ns re-equilibration simulation at 298 K. Random water molecules were replaced with K^+ and Cl^- ions to give an ion concentration of 140 mM. The hERG homology models were inserted into the bilayer using g_membed,[38] and the number of K^+/Cl^- ions was adjusted to maintain electroneutrality (the net protein charge is −4, and two K^+ ions were present in the selectivity filter as described above). Both simulation systems were energy minimized using steepest descent for 2000 steps and were then heated to 310 K for a further 5 ns simulation in which the non-hydrogen protein backbone atoms and selectivity filter K^+ ions were restrained. Production runs were performed for 500 ns using the OPLS all-atom forcefield,[39] Berger lipid parameters,[40] and the SPC water model.[41] Electrostatic interactions were modeled using the particle mesh Ewald algorithm,[42] and a cutoff of 10 Å was applied to van der Waals interactions. Bond lengths for protein and water were constrained using the LINCS and SETTLE algorithms, respectively.[43,44] The Nose−Hoover thermostat[45] was used to maintain the temperature at 310 K, while semi-isotropic pressure coupling was enabled through the

dx.doi.org/10.1021/ci4000739 | J. Chem. Inf. Model. 2013, 53, 1358−1370

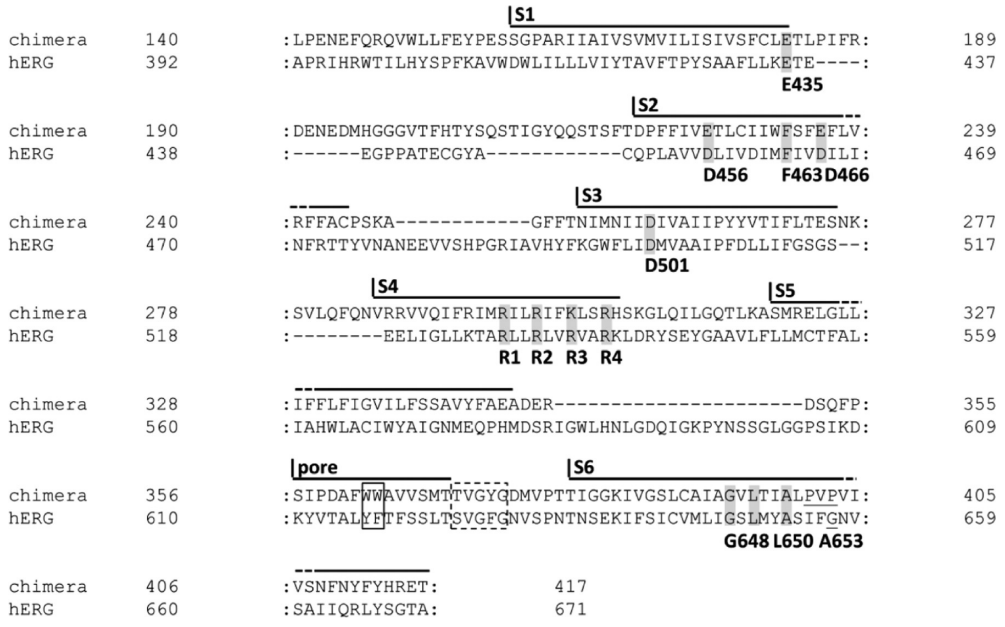

Figure 1. Sequence alignment between the hERG membrane domain and the Kv1.2/2.1 chimera used for hERG model construction. Key amino acid identities/similarities used in aligning transmembrane domains are shaded, and identities/similarities in the pore helix and selectivity filter used to align these regions are boxed. Sequence annotations based on Kv1.2/2.1 identify the approximate extent of transmembrane and pore helices, and key amino acids described in the text refer to hERG.

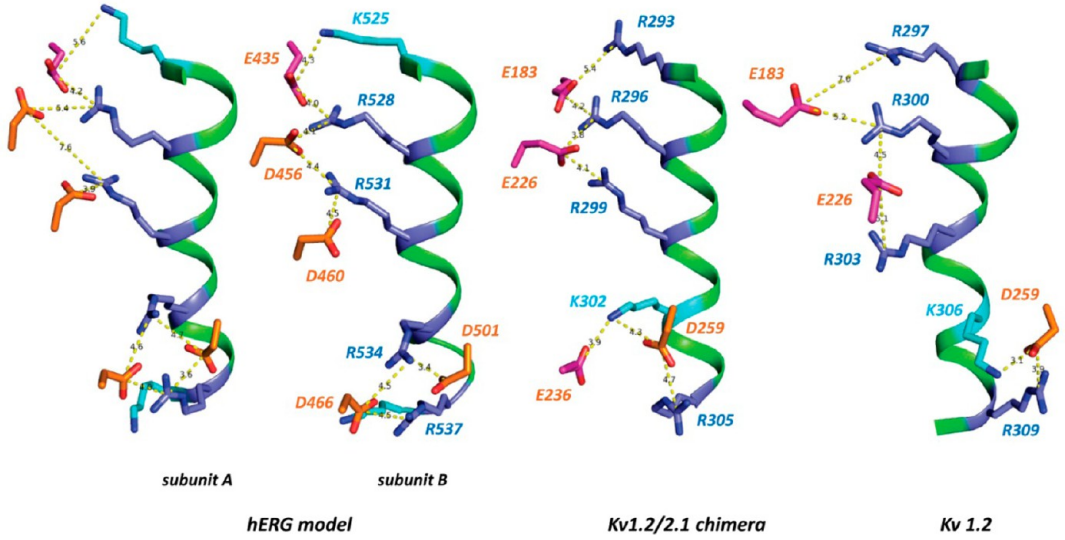

Figure 2. Comparison of charge-pairing interactions involving S4 residues in the hERG wild-type model with equivalent interactions in the X-ray structures of the Kv1.2/2.1 chimera[3] and Kv1.2.[4] The S4 helix of two subunits in the hERG wild-type model are shown following energy minimization before MD simulation, illustrating that some interconversion of charge pairing can occur simply by switching of side-chain rotamers, in this case of residues D456 and D460 in helix S1. Distances are in Å.

Parrinello–Rahman barostat.[46] Periodic boundary conditions were applied in all directions. No constraints were applied to the K^+ ions and water molecules in the selectivity filter. Simulations were performed with a time-step of 2 fs, and coordinates were saved every 100 ps. The first 30 ns of each simulation was considered to be an equilibration period; analysis of diagnostic parameters including distances between atom pairs and hydrogen bond occupancies was based on the final 470 ns of each simulation. Molecular dynamics simulations were performed using the high-performance computing facility at the University of Bristol Advanced Computing Research Centre.

RESULTS

Construction of Homology Model. There are several voltage-dependent potassium channels for which crystal structures have been determined.[1−4] The open-state mammalian channel structure having the most reliable structural relationship between voltage sensors and pore domain that was available at the time of model construction is the Kv1.2/2.1 chimera channel described by Long et al.[3] This chimera structure served as the template for construction of the hERG models described here. Full open-state homology models (S1−S6) of wild-type and L532P hERG channels including the

dx.doi.org/10.1021/ci4000739 | J. Chem. Inf. Model. 2013, 53, 1358−1370

extracellular S5−P linker were built onto the Kv1.2/2.1 template.

The sequence alignment used for model construction (Figure 1) was aided by the wealth of information on conserved residues within the potassium channel family. The C-terminal region of the template S1 helix contains a conserved glutamate at position 183 (E435 in hERG), the S2 helix has three highly conserved residues E226 (D456 in hERG), F233 (F463 in hERG), and E236 (D466 in hERG), while the S3 helix has a conserved aspartate at position 259 (D501 in hERG).[24] The four arginine residues in S4 (R1−R4 in Figure 1) were aligned on the basis of the similarity of the two hydrophobic residues separating them. These aspartate, glutamate, and arginine residues constitute sets of residue pairs involved in electrostatic interactions which stabilize the voltage-sensing domain in different channel states.[47] Conformational changes within voltage sensor domains (especially S4) that underlie channel gating involve a reorganization of the charge pairs as S4 moves in response to changes in membrane potential.[48] The spatial relationships between these residues in the open (activated) channel chimera template and the hERG model are illustrated in Figure 2. Experimental work by Zhang et al. supports a direct interaction between the side chains of residues D456 (S2) and R528 (S4) in hERG in activated channel states.[47] In accordance with this, analysis of the 0.5 μs wild-type and L532P simulations indicates an average of one persistent D456−R528 interaction per subunit (Figure 3). In other words

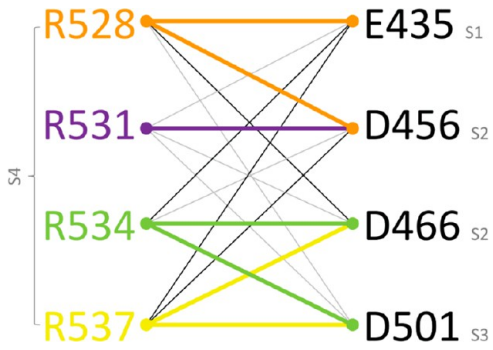

Figure 3. Potential pairwise electrostatic/hydrogen-bond interactions between charged residues in the S1/S2/S3 and S4 helices of WT and L532P hERG. Interactions are highlighted in color if the average number of interactions (Arg guanidine−Asp/Glu carboxylate H−O separation of ≤3.5 Å) was greater than 1 when averaged throughout the simulation (see text). Disallowed interactions (black lines) correspond to guanidine−carboxylate group separations of more than 5 Å in the starting structure. These interactions were not populated during the simulations. Five additional potential interactions that were not observed in any subunits during the simulations are indicated with gray lines.

at least one carboxylate oxygen atom of D456 was within 3.5 Å of a side-chain NH hydrogen of R528 averaged over the entire simulation. The variability in charge pairing interactions represented in Figure 3 results from the presence of some simultaneous pairing with two oppositely charged groups as also observed in crystal structures of voltage-dependent channels (e.g., Figure 2), and the observation that inter-conversion of side-chain rotamers can result in switching of charge-pair partners (Figure 2). The alignment in Figure 1 brings the side chains of S2 residues D456, D460 and D509 on S3 into proximity, consistent with the evidence that these constitute a Cd^{2+} binding site in hERG accessible from the extracellular surface (see Figure S3 in SI).[49]

Our model was built independently of that of Subbotina et al. who assessed hERG homology models built on the Kv1.2/2.1 chimera structure, with various alignments of the positively charged voltage-sensing arginine and lysine residues in S4.[22] Their preferred hERG+3 model for the S4 helix conforms to the alignment that we consider best accommodates the S4 motif described in the previous paragraph; the main difference with the Subbotina alignment is in the hERG S5 helix which has poor homology with the S5 transmembrane domains of other voltage-sensitive potassium channels (see below). From their hERG+3 model, Subbotina et al. predict a salt bridge between D501 (S3) and R534 (S4) which is present on average as one interaction per subunit throughout the 0.5 μs simulations performed in this study (Figures 2 and 3). Our alignment of S4 is also in agreement with the alignment of Lee et al.[24]

Given the lack of conserved residues in the S5 helix there is no consensus alignment for this helix, and several differing alignments have been described in the literature.[22,24,50,51] Since the S5 helix follows immediately after the S4−S5 linker, this helix was aligned by leaving no gaps between the end of S4 and the start of S5. In our model the S5 transmembrane helix starts near F551 and extends to around P577. Since the S5 helix lies at a shallow angle in the membrane, the helix extent is somewhat longer than the ∼20 residues required to span the membrane in more vertically oriented transmembrane helices of membrane proteins. The extent of the S5 helix in our model is similar to that described in the homology of Lee et al. (2009).[24] Ju et al. (2009) define the S5 helix as the sequence between F551 and A570, on the basis of NMR analysis of a micelle-associated synthetic peptide.[51] However, they also suggest that the following sequence (G572−P577) is in a helical conformation, and if this is considered to be an extension of the S5 helix, it brings the S5 helical extent between our model, the analysis of Ju et al., and the alignment of Lee et al. into broad agreement. Our S5 helix alignment also brings W568 close to T618 of the pore helix as suggested by functional analysis of inactivation in hERG mutants, although these residues are not in van der Waals contact in our model as suggested by Ferrer et al. (2011).[52] The point at which the S5 helix becomes the long S5−P linker is not easily defined since our modeling indicates that the N-terminal end of the linker is also helical; however there is a significant discontinuity between the C-terminal end of S5 and the N-terminal end of the S5−P linker which results in a bend of around 40° between the orientation of the S5 helix and that of the helical segment at the start of the S5−P linker.

The pore helices and selectivity filter were readily aligned, given the presence of the highly conserved two-residue aromatic amino acid motif (boxed in Figure 1) and conserved 'TVGYG' signature sequence. The S6 helix also contains a number of conserved residues: G394 (G648 in hERG),[32] L396 (L650 in hERG),[31] and A399 (A653 in hERG).[33] The template and model structures differ in S6 helical composition in that the Kv1.2/2.1 chimera contains a 'PxP motif' (PVP403), whereas hERG has a glycine at the equivalent position of P403 (IFG657) (Figure 1). Despite the presence of two proline residues, the structure of S6 remains broadly helical through the PVP sequence, and so the S6 helix in our model retains an overall helical conformation. Notably, the aromatic side chains of Y652 and F656 (that make dominant contributions to

dx.doi.org/10.1021/ci4000739 | J. Chem. Inf. Model. 2013, 53, 1358−1370

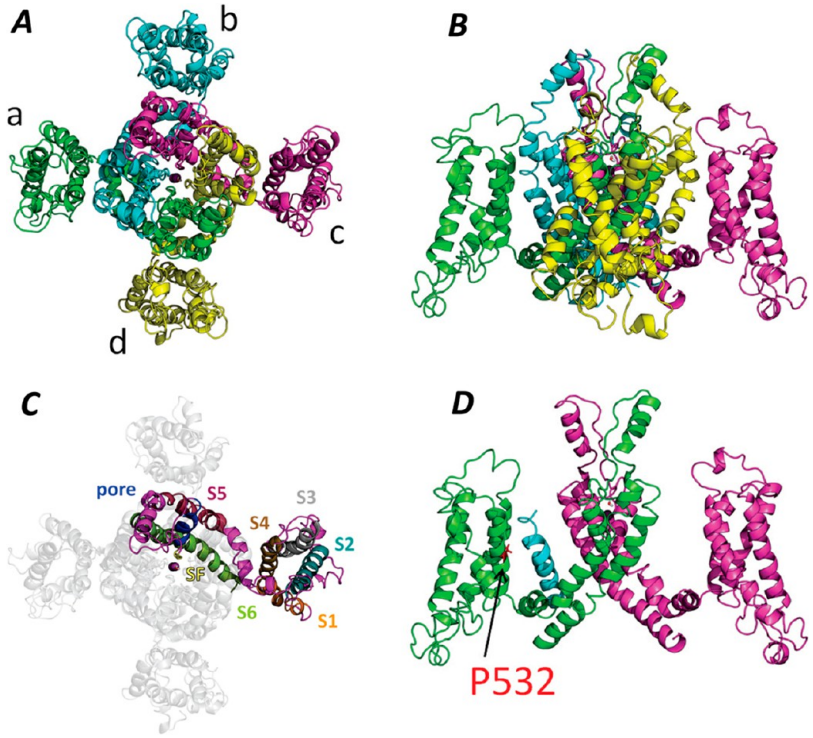

Figure 4. Structure of the wild-type and L532P hERG membrane domain model. (A) Top view (wild-type). (B) Side view (wild-type). (C) Identification of helical elements within a subunit of the hERG model annotated with transmembrane helix numbers for the voltage sensor (S1−S4) and pore (S5, S6) domains. SF denotes the selectivity filter. (D) L532P hERG model indicating the location of P532 in the S4 transmembrane helix (subunits b and d are omitted for clarity).

binding of many drugs that block hERG conductance) face the pore lumen where they are expected to be accessible for interaction with drug molecules, similar to the orientation of these amino acid side chains in homology models of the hERG pore used in docking analyses.[12−18]

Although there are no available template coordinates for the ∼40-amino-acid-long turret region and only limited information about its three-dimensional structure, its role in hERG rapid inactivation is well documented.[53,54] Given the effect of the L532P hERG mutation on inactivation kinetics,[27] we consider it useful to include the S5−P linker in our model so that this can be updated as experimental insight into the structure of S5−P evolves. Using CD spectropolarimetry and NMR spectroscopy, Torres et al. have shown that residues W585−I593 form an amphipathic helix in the presence of SDS micelles.[55] We therefore selected a 25-residue amino acid loop from a precomputed PDB subset database between template residues E349−Q353 (which encompasses S581−I607 in hERG) in which the following hERG sequence 'I583GWLHNLGDQIGK595' is contained within an α-helix. The structure of the full WT hERG membrane domain model is shown in Figure 4, and the experimental constraints used to construct and validate elements of the models are collated in Table S2 in SI.

Since the model of Subbotina et al.[22] (recently updated in Durdagi et al.)[23] constitutes the other currently available model for the full membrane domain of hERG in an open channel form, it is worth commenting on differences between their model and ours. The alignment of the hERG sequence with Kv1.2 and with the Kv1.2/2.1 chimera is equivalent in both models through the end of S4, and the models are broadly equivalent in the transmembrane regions within the voltage sensor. Likewise, the pore domain from the pore helix through to the end of S6 is likely to be similar in both models. The main difference lies in the region of the protein encompassing the S4−S5 linker and S5 helix of the pore domain. In the Subbotina/Durdagi model a five-residue segment of Kv1.2 (or Kv1.2/2.1 chimera), QTLKA (residues 315−319 of Kv1.2/2.1; see Figure 1) was omitted from the alignment truncating the S4−S5 linker and shifting the alignment of the S5 helix by 5 residues (i.e., the amino acid residues of the S5 helix in this model map onto amino acids five residues toward the C-terminus of the template sequences).[22,23] In our alignment, which retains the QTLKA sequence of the template structure, the amino acids of the S4−S5 linker fall naturally onto a strongly amphipathic helix in which the side chains of the charged amino acids D540, R541, and E544 project toward the cytoplasmic aqueous phase and the nonpolar side chains, in particular Y542 and Y545, project in the direction of the membrane interior where they interact with nonpolar side chains near the cytoplasmic ends of the S4 and S5 helices. The structure in this region of our model and the rotation of the S4−S5 helical linker with respect to the interfacial region of the cytoplasmic membrane leaflet is very similar to the NMR structure and rotation of the equivalent region of a peptide corresponding to residues 531−560 of hERG in a micelle.[56] However, there remains some uncertainty in the optimal alignment of hERG especially through the S5 helix, which is reflected in the difference in our model compared with that of Subbotina/Durdagi; this is unlikely to be resolved without a hERG crystal structure. It should also be noted that while the crystal structures of the Kv1.2/2.1 chimera and refined Kv1.2 channels are very similar, these may not constitute ideal templates for hERG in some regions of the structure. However,

dx.doi.org/10.1021/ci4000739 | J. Chem. Inf. Model. 2013, 53, 1358−1370

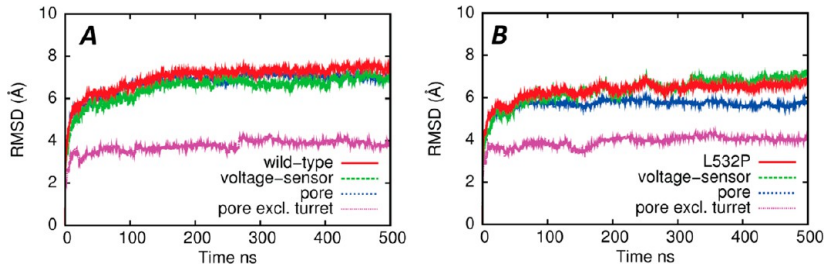

Figure 5. Backbone RMSD for individual elements of the hERG structures during 0.5 μs simulation in hydrated POPC bilayer patches are color coded. (A) Wild-type hERG model. (b) L532P hERG model.

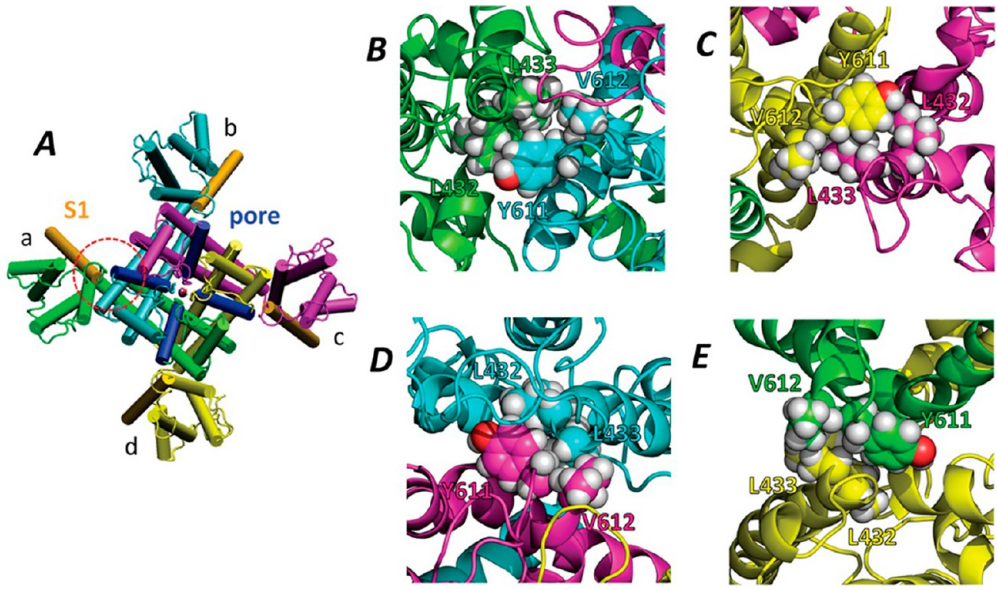

Figure 6. Persistent cluster of hydrophobic side chains comprising pore helix residues (Y611, V612) and residues in the voltage sensor domain near the top of S1 (L432, L433). (A) Overview of model structure identifying a close contact (circled) between the top of S1 (orange) and the N-terminal end of the pore helix of the pore domain (dark blue). The color coding is matched to the colors in panels B–E. (B) Wild-type hERG S1–pore helix interface involving subunits a and b, and (C) subunits c and d at 400 ns. (D) L532P S1–pore helix interface involving subunits b and c, and (E) subunits d and a at 300 ns.

the similarity of the voltage sensor domain in our model and open channel versions of the Subbotina/Durdagi model reflects the confidence in structural alignment supported by a significant number of charged-pair interactions in this domain of hERG (Figures 1-3).

Molecular Dynamics. The starting structures for the simulations described in this paper were constructed following a number of preliminary simulations to assess the optimal bilayer lipid model and K^+ ion loading of the selectivity filter (not shown). We found that the presence of K^+ ions in the selectivity filter stabilized the channel tetramer (even though some K^+ ions diffused from the selectivity filter during model runs), and hence these were included as described under Construction of Homology Model above.

All-atom root mean squared deviation (RMSD) curves from initial coordinates (Figure 5) for the wild-type and L532P mutant simulations indicate that the systems have largely equilibrated around local minima by 150 and 200 ns, respectively. Backbone heavy atom RMSD curves for the full protein (excluding selectivity filter K^+ ions and water molecules), voltage sensor domain, pore domain, and pore domain excluding the turret region are shown. For both wild-type and mutant channels the voltage-sensing and turret regions contribute most to the RMSD; the loops connecting transmembrane helices make the dominant contribution to RMSD in the voltage sensor domains (not shown).

The area per lipid in the wild-type and L532P hERG simulations is 64.5 Å^2 and 64.6 Å^2, respectively, which is in good agreement with available experimental values of POPC at 310 K of 66 Å^2 (ref 57) and 63 Å^2 (ref 58). GridMAT-MD was employed to calculate the thickness of the bilayer throughout the simulations by measuring the z-distance between the P8 atoms in the two membrane leaflets.[59] For the wild-type and L532P mutant channel systems the thickness of the POPC bilayer was 38.1 Å and 38.0 Å, respectively which is also in good agreement with an experimental value at 300 K of 37 Å (ref 60) and with several simulations using different force fields.[61]

Direct Interactions between S1 and Pore Helices of Adjacent Subunits. Interactions between voltage sensor and pore domains of voltage-sensitive channels are of fundamental interest since these interactions couple changes in membrane potential to channel gating. Recent analysis has provided evidence that interactions between residues near the extracellular end of S1 and the N-terminal end of the pore helix are important for channel function and may provide a fixed anchor point to facilitate coupling of conformational changes within the voltage sensor to the pore.[24] We inspected the models and trajectories for the presence of such interactions.

dx.doi.org/10.1021/ci4000739 | J. Chem. Inf. Model. 2013, 53, 1358–1370

In both the wild-type and L532P hERG models persistent interactions between the C-terminal end of S1 and the pore helix were maintained throughout the simulations. In both simulations two sets of interactions were represented. The first constitutes a hydrophobic cluster comprising L432 and L433 (top of S1) and Y611 and V612 (pore helix). Clustering of these side chains was maintained in all subunits in both wild-type and L532P simulations (Figures 6 and 7), although the

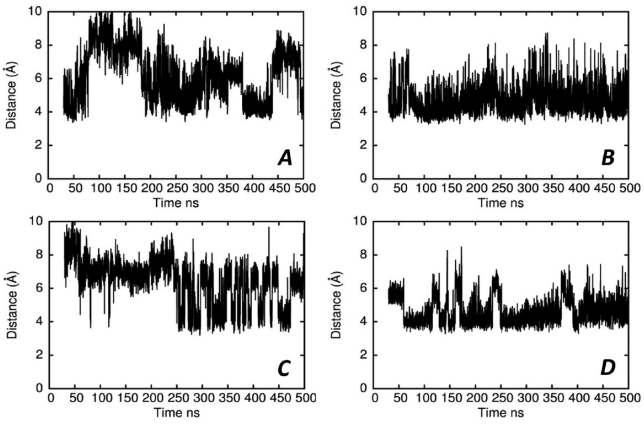

Figure 7. Time dependence of distances for representative interactions between pore helix residues and residues near the top of S1 illustrated in Figure 6. (A) Wild-type L432 Cδ2 (subunit a)/Y611 CZ (subunit b). (B) Wild-type L433 Cδ2 (subunit b)/Y611 CZ (subunit c). (C) L532P L433 Cδ2 (subunit c)/Y611 CZ (subunit d). (D) L532P L433 Cδ2 (subunit d)/ V612 Cγ1 (subunit a).

S1−pore helix interface was sufficiently fluid to allow interconversion of side-chain rotamers (Figure 7). In some cases the aromatic hydroxyl hydrogen of Y611 approached close enough to the S1 helical backbone to the hydrogen bond with the main-chain carbonyl of L432. This hydrophobic cluster is located within the relatively polar interfacial region between the lipid acyl chains and water phase above the bilayer.

The second set of interactions involves the glutamic acid side chains of E437 and E438 in the S1−S2 loop and K610 at the N-terminal end of the pore helix. These amino acids in our model reside in the aqueous phase just above the phospholipid headgroup interfacial region. In both simulations one of these glutamate side chains dominates interactions with K610 (E438/K610 interactions in wild-type; E437/K610 interactions in L532P), although swapping between E437 and E438 in interactions with K610 occurs during the simulations (Figure 8).

Voltage Sensor S4 helix and the Effects of an L532P Mutation. The most direct effect of mutation of L532 to proline is expected to be a perturbation of the S4 helix of the voltage sensor since proline is poorly tolerated in internal sites of polypeptide helices in the absence of stabilizing tertiary interactions. Analysis of S4 backbone hydrogen-bonding patterns, and backbone and side-chain conformations indicates that the S4 helix of hERG L532P remains largely intact during 0.5 μs of simulation. In both systems the S4 helix adopts a mixed $\alpha/3_{10}$ hydrogen-bonding pattern with 3_{10} helical hydrogen bonding predominating (Figure 9), consistent with the arrangement of positively charged side chains that form a "stripe" down the face of the helix that points into the voltage sensor domain (Figure 10). This overall helical geometry is maintained despite some loss of canonical hydrogen bonding in

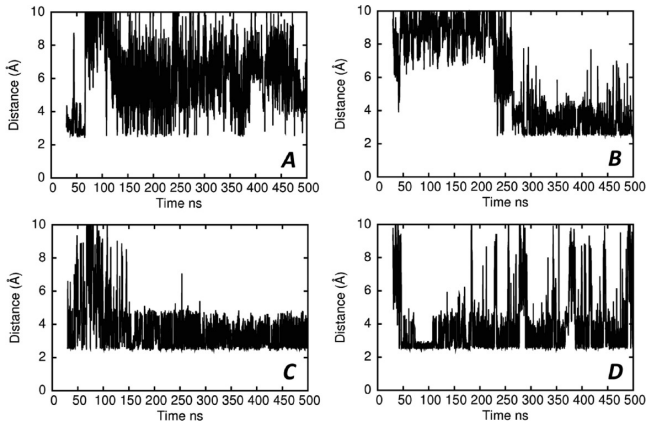

Figure 8. Time dependence of distances for representative electrostatic interactions between pore helix residue K610 and residues E437/E438 near the top of S1. (A) Wild-type E438 (subunit a)/K610 (subunit b). (B) Wild-type E437 (subunit c)/K610 (subunit d). (C) L532P E438 (subunit b)/K610 (subunit c). (D) L532P E437 (subunit d)/K610 (subunit a). Distances were measured between a glutamate side-chain oxygen (Oε1 or Oε2) and the lysine side-chain nitrogen (NZ).

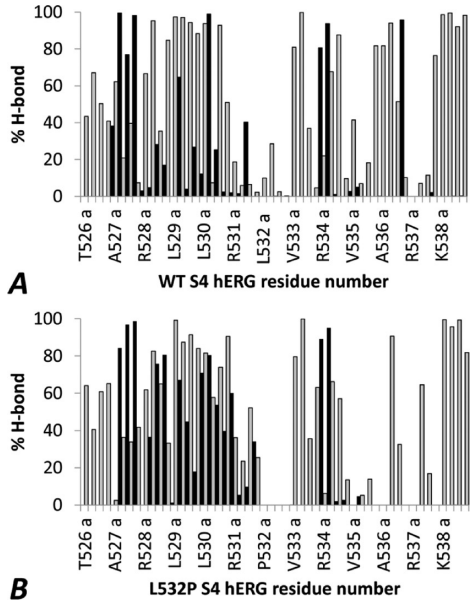

Figure 9. Hydrogen bond occupancies during 0.5 μs simulation for S4 hERG backbone amide NH groups. Panels A and B define the percentage of the total simulation time either α-helical (black) or 3_{10} helical (gray) hydrogen bonds involving the amide NH group of the residue indicated, were present for the wild-type and L532P model simulations, respectively. Data for each of the four subunits of each model are shown; for clarity only subunit a is labeled. A hydrogen bond is considered to be occupied if the N--O distance is $\leq$0.37, and the N−H--O angle is 180 $\pm$ 60°.

the C-terminal end of the S4 helices, particularly in L532P S4 (Figure 9). Notably, an overlay of the region of S4 containing the four arginine residues after 0.5 μs of simulation indicates that the S4 helix in the L532P mutation adopts a conformation with a tighter distribution of the four separate voltage sensor S4 helices than is found in the wild-type structure after 0.5 μs (Figure 10). As often found with proline-containing helical segments, the internal proline lies on the outside of a kink between the helical elements N- and C-terminal to the

dx.doi.org/10.1021/ci4000739 | J. Chem. Inf. Model. 2013, 53, 1358−1370

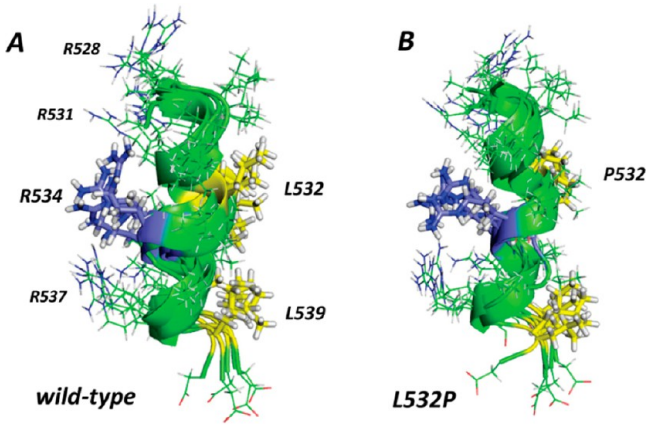

Figure 10. Overlay of S4 transmembrane helical segments of each subunit within wild-type and hERG L532P models after 0.5 μs molecular dynamics simulation. Clustering of selected side chains is identified including the "stripe" of arginine side chains on the internal face of S4. The helix face containing L532 (P532) and L539 is oriented toward S5 of the pore domain.

proline.[62] Since these structural features are represented in all four of the voltage sensor subunits in the L532P hERG simulation (Figure 10), we consider this to be a robust description of the effects of the L532P mutation on S4 helical structure. The proline residue and S4 helix kink are accommodated in the L532P voltage sensor domain as a result of persistent electrostatic interactions involving the S4 arginines and aspartate residues on helices S2 and S3 (see Figures 2 and 3).

Direct Interactions between Helices S4 and S5 and Effects of an L532P Mutation. During both wild-type and L532P mutant simulations the S4 and S5 helices of neighboring subunits remained in contact, especially in the region from around the membrane center to the extracellular membrane surface. We characterized several sets of potential interactions between amino acid side chains in S4 and S5, respectively. In the wild-type simulation we observe persistent hydrophobic contacts between the following pairs of S4/S5 residues; L529/I571, L532/A565, and L539/A561. In the L532P mutant the L529/I571 interaction is maintained, whereas A565 now forms contacts with V533 instead of L532. In both wild-type and L532P simulations L530 and V533 make contacts with Y569. These residues form a cluster of largely aliphatic side chains between the S4 and S5 helices that is more tightly packed in the wild-type structure compared to L532P (Figure 11), largely due to the loss of the bulky L532 side chain and the kinked structure of the L532P S4 helix which slightly reduces the S4–S5 contact surface throughout the mutant simulation. In addition to direct S4–S5 side-chain interactions, persistent contacts are made between tyrosine side chains Y542 and Y545 in the S4–S5 linker and H562 in S5 (Figure 11). Contacts between S4 and S5 are maintained throughout the 0.5 μs simulations supporting the interpretation that the S4 and S5 helices of neighboring subunits are in close contact in open states of the hERG channel, and together with the S4–S5 linker provide an additional means of connecting the two domains.

Lipid Infiltration between Voltage Sensor and Pore Domains. The accommodation of single tryptophan substitution mutants throughout the S4 helix has led to the suggestion that the S4 helix is loosely packed within the hERG structure and may be exposed to lipid.[63] To explore the integrity of voltage sensor–pore interactions on the microsecond time scale we inspected the simulations for examples of lipid infiltration between the voltage-sensing and pore domains. Although some periodic incursion of lipid acyl chains occurred into the regions between S4 and S5 where these are not closely apposed in the bilayer leaflet corresponding to the intracellular face of the membrane, there were no instances of separation of

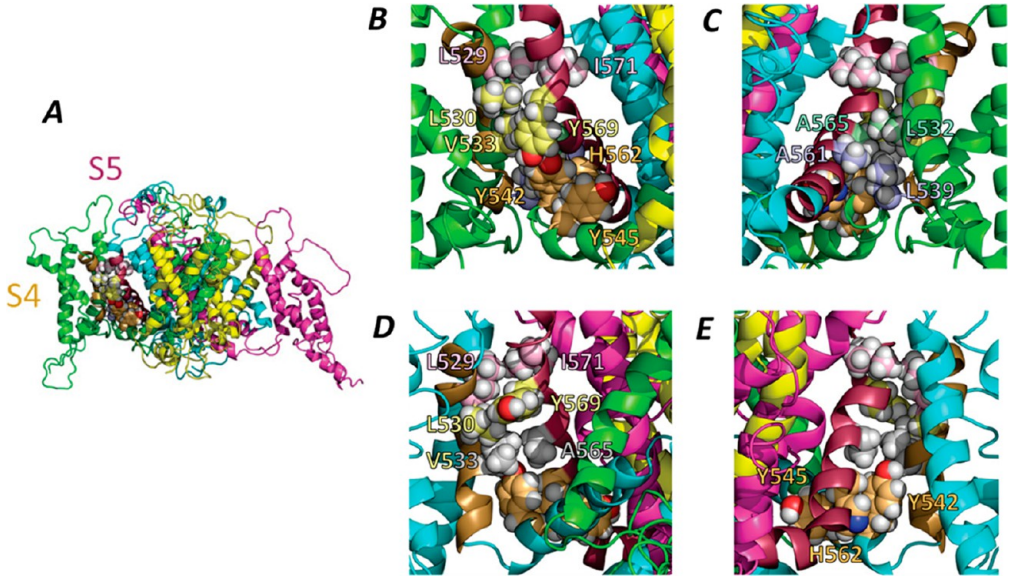

Figure 11. Persistent hydrophobic interactions between residues located at the interface between transmembrane helices S4 and S5. In each panel the residues of helices comprising the S4–S5 interface are colored gold (S4) and burgundy (S5), respectively. (A) Overview of wild-type model (500 ns simulation time) with color coding matched to the colors of the remaining panels. (B) Wild-type hERG with interface side-chain interactions involving L529–I571, L530/V533–Y569, L532–A565, L539–A561, and Y542/Y545–H562 of subunits a (S4) and b (S5); (C) 180° rotation of panel B; (D) L532P–hERG interactions involving L529–I571, L530–Y569, V533–A565 and Y542/Y545–H562 of subunits b (S4) and c (S5); (E) 180° rotation of panel D.

dx.doi.org/10.1021/ci4000739 | J. Chem. Inf. Model. 2013, 53, 1358–1370

voltage sensor and pore domains by diffusion of phospholipid molecules between S4 and S5 helices [see movies in SI]. Phospholipids in protein-free regions of the bilayer underwent diffusion of up to 5 nm in the plane of the membrane during 0.5 μs simulation (Figure S4 in SI), equivalent to approximately 4−5 lipid diameters, indicating that lipid diffusion between S4 and S5 helices is possible on the time scale of the simulations. The absence of phospholipid incursions in any of the four subunit pairs in either WT or L532P simulations (4 μs total simulation time) supports the interpretation that interactions between S4 and S5 are stable on the microsecond time scale.

DISCUSSION

In voltage-sensitive Na^+ and K^+ ion channels the voltage sensor and pore domains within each subunit are connected by a short largely helical linker (S4−S5 linker) between the voltage sensor S4 transmembrane helix and the S5 helix of the pore domain on the intracellular side of the membrane. The pore domain itself interacts not only with the pore domains of adjacent subunits but also with the voltage sensor of the following subunit in an anticlockwise direction. This interdigitation of specific elements of the channel subunits is likely to maintain structural integrity in channel structure and to promote a concerted response of voltage sensor and pore domains to the changes in membrane potential that underlie channel gating.

Our simulations demonstrate that construction of hERG models onto the Kv1.2/2.1 chimera crystal structure results in open channel states that are stable to molecular dynamics simulation in a fully hydrated POPC membrane model on the 0.5 μs time scale, retaining the broad structural features that characterize the domain organization of voltage sensitive ion channels. By comparison with experimental data on the state dependence of side-chain accessibility and mutant cycle analysis,[47,64] the pattern of charge interactions between arginine and lysine residues on S4 and aspartic acid residues on the S2 and S3 helices (Figures 2 and 3) establish that the voltage sensor domain is in an open (or open-inactivated)-state conformation that interfaces with the open state of the pore domain. Four main conclusions may be made from analysis of the simulation trajectories. First, the hERG models identify persistent interactions involving residues at the top of S1 and the N-terminal end of the pore helix that may anchor nonmobile elements of the voltage sensor domain. Second, the simulations support the conclusion that a direct interaction surface between the S4 helix of the voltage sensor domain and the S5 helix of the pore domain may modulate the gating properties of hERG. Third, accommodation of the L532P mutation in a stable S4 helix provides an explanation for the retention of functional channels in this mutation.[27] Fourthly, a perturbation of the S4−S5 interface in the L532P mutant model suggests an explanation for the greatly enhanced channel deactivation kinetics observed experimentally (Table S1 in SI).[27] These interpretations are discussed in the following sections.

Anchoring Interactions between Voltage Sensor Domain and Pore Helix. In addition to the S4−S5 linker, Lee et al. (2009) have identified an interface in voltage sensitive K^+ channels between the voltage sensor and the pore domain involving residues at the extracellular surface of S1 and the N-terminal end of the pore helix of the adjacent subunit.[24] Since our model is built onto the structure of the Kv1.2/2.1 chimera in which this interface is represented, it is not surprising that a similar interface is found in the starting structure of the model. In X-ray structures of related K^+ channels including Kv1.2 and the Kv1.2/2.1 chimera,[3,4] stabilizing interactions between S1 and pore helix residues involve hydrogen-bond interactions within a cluster of evolutionarily conserved amino acids.[24] hERG does not share this sequence conservation at the top of the pore helix (see Figure S2 in SI), and although T436 in hERG aligns with one of the conserved set of residues at the top of S1 (T184 in the chimera; Figure 1), this residue in our simulations did not participate in hydrogen-bond interactions with the backbone at the N-terminal end of the pore helix as observed in the crystal structures. Instead a persistent cluster of nonpolar side chains involving residues L432, L433 (top of S1) and Y611, V612 (N-terminal end of pore helix) constitutes the stable element of the interface in our models, with some additional electrostatic interactions involving glutamic acid residues (E437, E438) near the start of the loop connecting S1 and S2 and K610 of the pore helix. The stability of the hydrophobic cluster is probably a consequence of its location in the relatively polar headgroup region of the extracellular membrane leaflet where nonpolar interactions are expected to be promoted. Polymorphisms involving missense mutation of several residues in (or near) this hydrophobic cluster (Y611H, V612L, A614 V) result in long QT syndrome, attesting to the importance of interactions involving the N-terminal end of the hERG pore helix.[65,66] On the other hand a hERG construct in which both E437 and E438 are mutated to alanine shows little perturbation of gating or conductance,[49] indicating that interactions of these residues with K610 of the pore helix are not important for maintaining a functional interface. In the context of our models the hydrophobic cluster involving L432, L433, Y611, and V612 dominates the stability of this interface, whereas the electrostatic interactions involving E437, E438, and K610 result from the juxtaposition of these side chains arising from the stability of the adjacent hydrophobic cluster.

The S4−S5 Interface. The S4 transmembrane helix of the voltage sensor domain lies close to the S5 helix of the pore domain of the preceding subunit in the chimera, and this may provide an additional link between the voltage sensor and pore domain (see also ref 67). In our model, the close approach of S4 and S5 constitutes an interaction surface composed largely of aliphatic side chains encompassing residues in the sequence L529-L539 on one face of the S4 helix with residues in the sequence A561 to I571 on the opposing face of the S5 helix. During 0.5 μs simulation of both wild-type and L532P mutant channels this interaction surface is broadly maintained despite some differences in the pairwise interactions between S4 and S5 in L532P hERG compared to the wild-type simulation (Figure 11). However, the S4−S5 contact surface area is reduced in L532P hERG due to the smaller projection of the proline side chain from the S4 helix surface compared to leucine, and the proline-induced kink in the helix.

The nature of the interacting side chains at the S4−S5 interface may give some insight into an apparent incompatibility with the conclusion from systematic Trp replacements throughout the hERG S4 transmembrane domain that the S4 helix is loosely packed within the channel structure and may be lipid exposed.[63] These authors found that each of the residues in S4 in the sequence L524 - L539 that lie on the potential interface with S5 can be substituted with Trp while retaining channel function (although with significant effects on channel gating in many cases), suggesting that their side chains may not make defined interactions with amino acids in other channel domains. These observations (an interaction surface between

S4 and S5 that is maintained on the μs time scale, but which is tolerant to systematic Trp replacement) may be reconciled by the observation that this surface in our model consists largely of aliphatic side chains whose interactions may resemble those in molten globule states of partially folded proteins in which nonpolar side chains cluster without making the defined interactions that characterize close-packed folded states.[68] Such an interpretation is consistent with the observation that L529 that lies on the interface between S4 and S5 in our model can be replaced by Trp with only small effects on steady-state activation and activation/inactivation rates,[63] whereas an L529A mutation renders the hERG channel nonexpressible.[67] In other words the interface may be weakly discriminating of side chains so long as these are nonpolar and sufficiently bulky to fill volume in the interface between voltage sensor and pore domains. The nature of the S4−S5 interface in different channel states may contribute more generally to the specific gating properties of potassium channels. For example, tryptophan scanning mutagenesis has identified clusters of interacting amino acid side chains that map to the interface between S4 and S5 in the Shaker K^+ channel and whose mutation perturbs channel gating.[69]

Effect of L532P Mutation. Although internal proline residues disfavor helical conformations and stability, the L532P mutant retains channel function but with altered voltage-responsive gating (Figure S1 in SI),[27] and this is consistent with the observation that the L532P model retains much of the structural integrity in voltage sensor domain structure and voltage sensor - pore interactions that is present in the wild-type model in μs-scale simulations. The P532 residue is accommodated in a kinked S4 helix with some loss of canonical hydrogen bonding, but the overall (3_{10}) helical conformation is maintained by persistent electrostatic interactions between the voltage-sensing arginine residues and negatively charged side chains within the voltage sensor (Figures 9 and 10). Apart from effects on the voltage-dependence of activation and inactivation gating, the most marked effect of the L532P mutation on hERG channel function is to greatly increase the rate of channel deactivation (see Figure S1 and Table S1 in SI), indicating a reduced thermodynamic barrier for the transition from open to closed states.[27] Inspection of open-state models can only give insight into possible interactions in transition states to the extent that these are present in the open state. However, the interactions at the interface between S4 and S5 involving aliphatic side chains may stabilize the open state and oppose the movement of S4 toward the cytoplasmic side of the membrane in response to a repolarizing potential. Reduced coupling between S4 and S5 in the open state in L532P hERG by perturbation of this interface (Figure 11) would facilitate repolarization-induced conformational excursions of S4. In this scenario, the replacement of L532 with tryptophan has little effect on the kinetics of channel closing[63] because the bulky indole side chain can replace leucine to maintain stabilizing van der Waals contact at the S4−S5 interface. In support of this interpretation, fluorescence labeling of hERG residues that facilitates simultaneous assessment of the kinetics of S4 movement in response to changes in membrane potential and the corresponding kinetics of channel gating indicates that S4 moves rapidly in response to membrane depolarization and in advance of the conformational changes associated with pore opening,[70,71] whereas the slow time course for deactivation and S4 movement are more closely linked,[70] suggesting that the slow deactivation in hERG may be associated with slow transition of S4 from its open-state configuration. The observation that some mutations at the putative S4−S5 interface in the Shaker K^+ channel (e.g., F401A)[69,72] similarly strongly accelerate channel closing suggests that interactions at this interface may act more generally to modulate inactivation kinetics in K^+ channels (see also ref 73).

CONCLUSIONS

The simulations provide an explanation for the retention of membrane expression and gated (but altered) channel conductance in hERG L532P, since this potentially disruptive mutation is accommodated within a stable voltage-sensing domain that becomes partly uncoupled from the pore domain, consistent with large effects on gating kinetics observed experimentally. The S4−S5 interface and S4−S5 linker together likely constitute a motif that couples the gating response of the pore to voltage sensor movement, such that perturbations throughout the motif give rise to effects on gating response. Thus, mutagenesis of residues in and around the S4−S5 interface and interactions with the hERG N-terminal cytoplasmic domain that may be mediated through the S4−S5 linker (reviewed in ref 74) all modulate the gating response in otherwise functionally competent channels. The simulations also indicate that pairwise comparison of mutant and wild-type channel models is a useful approach to the structural basis of functional effects of mutation even when some uncertainty exists in the model. This approach may provide a starting point for model refinement in conjunction with experimental analysis informed by modeling and dynamics simulation. The simulation times in fully atomistic models are insufficient to explore large-scale movement involving, for example, responses to changes in membrane potential that occur on the millisecond time scale.[71] However, the observation of facile charge movement resulting from changes in side-chain rotamer distributions (Figure 2) suggests that some of the early events in gating charge movement might be accessible to simulation in response to changes in membrane potential.

ASSOCIATED CONTENT

Supporting Information

A summary of the electrophysiological characterization of the L532P hERG mutation in comparison with the wild-type hERG channel when expressed in human embryonic kidney (HEK) cells. Current−voltage relationships are shown in **Figure S1** and the biophysical parameters of the channels are summarized in **Table S1**. **Table S2** collates the constraints and interactions used to construct homology models and the key sets of interactions identified in the simulations. **Figure S2**: sequence homology between closely related mammalian voltage-dependent K^+ channels; **Figure S3**: spatial relationship of aspartic acid residues within the voltage sensing domain; **Figure S4**: examples of lipid diffusion during simulation trajectories. **Videos** ci4000739_si_002.mpg and ci4000739_si_003.mpg: time evolution of the membrane water interface during molecular dynamics simulation for WT and L532P hERG models. A description of the videos. This material is available free of charge via the Internet at http://pubs.acs.org.

AUTHOR INFORMATION

Corresponding Author

*E-mail: c.dempsey@bristol.ac.uk. Tel.: (0)117 3312134. Fax: (0)117 3312168.

Notes

The authors declare no competing financial interest.

■ ACKNOWLEDGMENTS

The work was funded by BBSRC (UK) through a PhD studentship to C.K.C., the British Heart Foundation (Grants PG 06/042 and PG 10/017), and the University of Bristol via provision of the high performance computing through the Advanced Computing Research Centre (http://www.acrc.bris.ac.uk). We are grateful to Dr. Nathalie Reuter of the Computational Biology Unit, University of Bergen for helpful insight into longer time scale dynamics in our models, and the World University Network (WUN) for a travel grant.

■ ABBREVIATIONS

hERG, human Ether-à-go-go-Related Gene; MD, molecular dynamics; POPC, 1-palmitoyl-2-oleoyl-*sn*-glycero-3-phosphocholine

■ REFERENCES

(1) Jiang, Y.; Lee, A.; Chen, J.; Ruta, V.; Cadene, M.; Chait, B. T.; MacKinnon, R. X-ray structure of a voltage-dependent K^+ channel. *Nature* **2003**, *423*, 33−41.

(2) Long, S. B.; Campbell, E. B.; Mackinnon, R. Crystal structure of a mammalian voltage-dependent Shaker family K^+ channel. *Science* **2005**, *309*, 897−903.

(3) Long, S. B.; Tao, X.; Campbell, E. B.; MacKinnon, R. Atomic structure of a voltage-dependent K^+ channel in a lipid membrane-like environment. *Nature* **2007**, *450*, 376−382.

(4) Chen, X.; Wang, Q.; Ni, F.; Ma, J. Structure of the full-length Shaker potassium channel Kv1.2 by normal-mode-based X-ray crystallographic refinement. *Proc. Natl. Acad. Sci. U.S.A.* **2010**, *107*, 11352−11357.

(5) Cuello, L. G.; Jogini, V.; Cortes, D. M.; Perozo, E. Structural mechanism of C-type inactivation in K^+ channels. *Nature* **2010**, *466*, 203−208.

(6) Delemotte, L.; Tarek, M.; Klein, M. L.; Amaral, C.; Treptow, W. Intermediate states of the Kv1.2 voltage sensor from atomistic molecular dynamics simulations. *Proc. Natl. Acad. Sci. U.S.A.* **2011**, *108*, 6109−6114.

(7) Schow, E. V.; Freites, J. A.; Nizkorodov, A.; White, S. H.; Tobias, D. J. Coupling between the voltage-sensing and pore domains in a voltage-gated potassium channel. *Biochim. Biophys. Acta* **2012**, *1818*, 1726−1736.

(8) Hoshi, T.; Armstrong, C. M. Initial steps in the opening of a Shaker potassium channel. *Proc. Natl. Acad. Sci. U.S.A.* **2012**, *109*, 12800−12804.

(9) Law, R. J.; Capener, C.; Baaden, M.; Bond, P. J.; Campbell, J.; Patargias, G.; Arinaminpathy, Y.; Sansom, M. S. P. Membrane protein structure quality in molecular dynamics simulation. *J. Mol. Graphics Modell.* **2005**, *24*, 157−165.

(10) Stansfeld, P. J.; Sansom, M. S. P. From Coarse Grained to Atomistic: A Serial Multiscale Approach to Membrane Protein Simulations. *J. Chem. Theory Comput.* **2011**, *7*, 1157−1166.

(11) Sanguinetti, M. C.; Tristani-Firouzi, M. hERG potassium channels and cardiac arrhythmia. *Nature* **2006**, *440*, 463−469.

(12) Mitcheson, J. S.; Chen, J.; Lin, M.; Culberson, C.; Sanguinetti, M. C. A structural basis for drug-induced long QT syndrome. *Proc. Natl. Acad. Sci. U.S.A.* **2000**, *97*, 12329−12333.

(13) Witchel, H. J.; Dempsey, C. E.; Sessions, R. B.; Perry, M.; Milnes, J. T.; Hancox, J. C.; Mitcheson, J. S. The low-potency, voltage-dependent hERG blocker propafenone-molecular determinants and drug trapping. *Mol. Pharmacol.* **2004**, *66*, 1201−1212.

(14) Sanguinetti, M. C.; Mitcheson, J. S. Predicting drug-hERG channel interactions that cause acquired long QT syndrome. *Trends Pharmacol. Sci.* **2005**, *26*, 119−124.

(15) Farid, R.; Day, T.; Friesner, R. A.; Pearlstein, R. A. New insights about hERG blockade obtained from protein modeling, potential energy mapping, and docking studies. *Bioorg. Med. Chem.* **2006**, *14*, 3160−3173.

(16) Stansfeld, P. J.; Gedeck, P.; Gosling, M.; Cox, B.; Mitcheson, J. S.; Sutcliffe, M. J. Drug block of the hERG potassium channel: insight from modeling. *Proteins* **2007**, *68*, 568−580.

(17) Imai, Y. N.; Ryu, S.; Oiki, S. Docking model of drug binding to the human ether-a-go-go potassium channel guided by tandem dimer mutant patch-clamp data: a synergic approach. *J. Med. Chem.* **2009**, *52*, 1630−1638.

(18) El Harchi, A.; Zhang, Y. H.; Hussein, L.; Dempsey, C. E.; Hancox, J. C. Molecular determinants of hERG potassium channel inhibition by disopyramide. *J. Mol. Cell. Cardiol.* **2012**, *52*, 185−195.

(19) Durdagi, S.; Duff, H. J.; Noskov, S. Y. Combined receptor and ligand-based approach to the universal pharmacophore model development for studies of drug blockade to the hERG1 pore domain. *J. Chem. Inf. Model.* **2011**, *51*, 463−474.

(20) Kutteh, R.; Vandenberg, J. I.; Kuyucak, S. Molecular dynamics and continuum electrostatics studies of inactivation in the hERG potassium channel. *J. Phys. Chem. B* **2007**, *111*, 1090−1098.

(21) Stansfeld, P. J.; Grottesi, A.; Sands, Z. A.; Sansom, M. S.; Gedeck, P.; Gosling, M.; Cox, B.; Stanfield, P. R.; Mitcheson, J. S.; Sutcliffe, M. J. Insight into the mechanism of inactivation and pH sensitivity in potassium channels from molecular dynamics simulations. *Biochemistry* **2008**, *47*, 7414−7422.

(22) Subbotina, J.; Yarov-Yarovoy, V.; Lees-Miller, J.; Durdagi, S.; Guo, J. Q.; Duff, H. J.; Noskov, S. Y. Structural refinement of the hERG1 pore and voltage-sensing domains with ROSETTA-membrane and molecular dynamics simulations. *Proteins: Struct., Funct., Bioinf.* **2010**, *78*, 2922−2934.

(23) Durdagi, S.; Deshpande, S.; Duff, H. J.; Noskov, S. Y. Modeling of open, closed, and open-inactivated states of the hERG1 channel: structural mechanisms of the state-dependent drug binding. *J. Chem. Inf. Model.* **2012**, *52*, 2760−2774.

(24) Lee, S. Y.; Banerjee, A.; MacKinnon, R. Two separate interfaces between the voltage sensor and pore are required for the function of voltage-dependent K^+ channels. *PLoS Biol* **2009**, *7*, e1000047.

(25) Sessions, R. B.; Gibbs, N.; Dempsey, C. E. Hydrogen bonding in helical polypeptides from molecular dynamics simulations and amide hydrogen exchange analysis: Alamethicin and melittin in methanol. *Biophys. J.* **1998**, *74*, 138−152.

(26) Hassel, D.; Scholz, E. P.; Trano, N.; Friedrich, O.; Just, S.; Meder, B.; Weiss, D. L.; Zitron, E.; Marquart, S.; Vogel, B.; Karle, C. A.; Seemann, G.; Fishman, M. C.; Katus, H. A.; Rottbauer, W. Deficient zebrafish ether-a-go-go-related gene channel gating causes short-QT syndrome in zebrafish reggae mutants. *Circulation* **2008**, *117*, 866−875.

(27) Zhang, Y. H.; Colenso, C. K.; Sessions, R. B.; Dempsey, C. E.; Hancox, J. C. The hERG K(+) channel S4 domain L532P mutation: characterization at 37 °C. *Biochim. Biophys. Acta* **2011**, *1808*, 2477−2487.

(28) Larkin, M. A.; Blackshields, G.; Brown, N. P.; Chenna, R.; McGettigan, P. A.; McWilliam, H.; Valentin, F.; Wallace, I. M.; Wilm, A.; Lopez, R.; Thompson, J. D.; Gibson, T. J.; Higgins, D. G. Clustal W and Clustal X version 2.0. *Bioinformatics* **2007**, *23*, 2947−2948.

(29) Goujon, M.; McWilliam, H.; Li, W.; Valentin, F.; Squizzato, S.; Paern, J.; Lopez, R. A new bioinformatics analysis tools framework at EMBL-EBI. *Nucleic Acids Res.* **2010**, *38*, W695−W699.

(30) Hofmann, K.; Stoffel, W. TMbase - A database of membrane spanning proteins segments. *Biol. Chem. Hoppe Seyler* **1993**, *374*, 166.

(31) Li-Smerin, Y.; Hackos, D. H.; Swartz, K. J. A localized interaction surface for voltage-sensing domains on the pore domain of a K^+ channel. *Neuron* **2000**, *25*, 411−423.

(32) Osterberg, F.; Aqvist, J. Exploring blocker binding to a homology model of the open hERG K^+ channel using docking and molecular dynamics methods. *FEBS Lett.* **2005**, *579*, 2939−2944.

(33) Stepanovic, S. Z.; Potet, F.; Petersen, C. I.; Smith, J. A.; Meiler, J.; Balser, J. R.; Kupershmidt, S. The evolutionarily conserved residue

A653 plays a key role in hERG channel closing. *J. Physiol.* **2009**, *587*, 2555−2566.
(34) Aqvist, J.; Luzhkov, V. Ion permeation mechanism of the potassium channel. *Nature* **2000**, *404*, 881−884.
(35) Laskowski, R. A.; Macarthur, M. W.; Moss, D. S.; Thornton, J. M. Procheck - a program to check the stereochemical quality of protein structures. *J. Appl. Crystallogr.* **1993**, *26*, 283−291.
(36) Hess, B.; Kutzner, C.; van der Spoel, D.; Lindahl, E. GROMACS 4: Algorithms for highly efficient, load-balanced, and scalable molecular simulation. *J. Chem. Theory Comput.* **2008**, *4*, 435−447.
(37) Tieleman, D. P. *Biocomputing*. http://moose.bio.ucalgary.ca/index.php?page=Structures_and_Topologies (accessed April 30, 2013).
(38) Wolf, M. G.; Hoefling, M.; Aponte-Santamaria, C.; Grubmuller, H.; Groenhof, G. g_membed: Efficient insertion of a membrane protein into an equilibrated lipid bilayer with minimal perturbation. *J. Comput. Chem.* **2010**, *31*, 2169−2174.
(39) Jorgensen, W. L.; Tirado-Rives, J. The OPLS potential functions for proteins - energy minimizations for crystals of cyclic-peptides and crambin. *J. Am. Chem. Soc.* **1988**, *110*, 1657−1666.
(40) Berger, O.; Edholm, O.; Jahnig, F. Molecular dynamics simulations of a fluid bilayer of dipalmitoylphosphatidylcholine at full hydration, constant pressure, and constant temperature. *Biophys. J.* **1997**, *72*, 2002−2013.
(41) Berendsen, H.; Postma, J. P. M.; van Gunsteren, W. F.; Hermans, J. Interaction models for water in relation to protein hydration. In *Intermolecular Forces*; Pullman, B., Ed.; Reidel: Dordrecht, 1981; pp 331−342.
(42) Essmann, U.; Perera, L.; Berkowitz, M. L.; Darden, T.; Lee, H.; Pedersen, L. G. A smooth particle mesh Ewald method. *J. Chem. Phys.* **1995**, *103*, 8577−8593.
(43) Hess, B.; Bekker, H.; Berendsen, H. J. C.; Fraaije, J. G. E. M. LINCS: A linear constraint solver for molecular simulations. *J. Comput. Chem.* **1997**, *18*, 1463−1472.
(44) Miyamoto, S.; Kollman, P. A. Settle - an analytical version of the shake and rattle algorithm for rigid water models. *J. Comput. Chem.* **1992**, *13*, 952−962.
(45) Hoover, W. G. Canonical dynamics - equilibrium phase-space distributions. *Phys. Rev. A* **1985**, *31*, 1695−1697.
(46) Parrinello, M.; Rahman, A. Polymorphic transitions in single-crystals - a new molecular-dynamics method. *J. Appl. Phys.* **1981**, *52*, 7182−7190.
(47) Zhang, M.; Liu, J.; Jiang, M.; Wu, D. M.; Sonawane, K.; Guy, H. R.; Tseng, G. N. Interactions between charged residues in the transmembrane segments of the voltage-sensing domain in the hERG channel. *J. Membr. Biol.* **2005**, *207*, 169−181.
(48) Zhang, X.; Ren, W. L.; DeCaen, P.; Yan, C. Y.; Tao, X.; Tang, L.; Wang, J. J.; Hasegawa, K.; Kumasaka, T.; He, J. H.; Wang, J. W.; Clapham, D. E.; Yan, N. Crystal structure of an orthologue of the NaChBac voltage-gated sodium channel. *Nature* **2012**, *486*, 130−134.
(49) Fernandez, D.; Ghanta, A.; Kinard, K. I.; Sanguinetti, M. C. Molecular mapping of a site for Cd^{2+}-induced modification of human ether-à-go-go-related gene (hERG) channel activation. *J. Physiol.* **2005**, *567*, 737−755.
(50) Stary, A.; Wacker, S. J.; Boukharta, L.; Zachariae, U.; Karimi-Nejad, Y.; Aqvist, J.; Vriend, G.; de Groot, B. L. Toward a consensus model of the hERG potassium channel. *ChemMedChem* **2010**, *5*, 455−467.
(51) Ju, P.; Pages, G.; Riek, R. P.; Chen, P. C.; Torres, A. M.; Bansal, P. S.; Kuyucak, S.; Kuchel, P. W.; Vandenberg, J. I. The pore domain outer helix contributes to both activation and inactivation of the hERG K^+ channel. *J. Biol. Chem.* **2009**, *284*, 1000−1008.
(52) Ferrer, T.; Cordero-Morales, J. F.; Arias, M.; Ficker, E.; Medovoy, D.; Perozo, E.; Tristani-Firouzi, M. Molecular coupling in the human ether-a-go-go-related gene-1 (hERG1) K^+ channel inactivation pathway. *J. Biol. Chem.* **2011**, *286*, 39091−39099.
(53) Dun, W.; Jiang, M.; Tseng, G. N. Allosteric effects of mutations in the extracellular S5-P loop on the gating and ion permeation properties of the hERG potassium channel. *Pflugers Arch.* **1999**, *439*, 141−149.
(54) Liu, J.; Zhang, M.; Jiang, M.; Tseng, G. N. Structural and functional role of the extracellular S5-P linker in the hERG potassium channel. *J. Gen. Physiol.* **2002**, *120*, 723−737.
(55) Torres, A. M.; Bansal, P. S.; Sunde, M.; Clarke, C. E.; Bursill, J. A.; Smith, D. J.; Bauskin, A.; Breit, S. N.; Campbell, T. J.; Alewood, P. F.; Kuchel, P. W.; Vandenberg, J. I. Structure of the hERG K^+ channel S5P extracellular linker: role of an amphipathic alpha-helix in C-type inactivation. *J. Biol. Chem.* **2003**, *278*, 42136−42148.
(56) Ng, C. A.; Perry, M. D.; Tan, P. S.; Hill, A. P.; Kuchel, P. W.; Vandenberg, J. I. The S4−S5 linker acts as a signal integrator for hERG K^+ channel activation and deactivation gating. *PLoS One* **2012**, *7*, e31640.
(57) Hyslop, P. A.; Morel, B.; Sauerheber, R. D. Organization and interaction of cholesterol and phosphatidylcholine in model bilayer membranes. *Biochemistry* **1990**, *29*, 1025−1038.
(58) Smaby, J. M.; Momsen, M. M.; Brockman, H. L.; Brown, R. E. Phosphatidylcholine acyl unsaturation modulates the decrease in interfacial elasticity induced by cholesterol. *Biophys. J.* **1997**, *73*, 1492−1505.
(59) Allen, W. J.; Lemkul, J. A.; Bevan, D. R. GridMAT-MD: a grid-based membrane analysis tool for use with molecular dynamics. *J. Comput. Chem.* **2009**, *30*, 1952−1958.
(60) Kucerka, N.; Tristram-Nagle, S.; Nagle, J. F. Structure of fully hydrated fluid phase lipid bilayers with mono-unsaturated chains. *J. Membr. Biol.* **2005**, *208*, 193−202.
(61) Piggot, T. J.; Piñeiro, A.; Khalid, S. Molecular dynamics simulations of phosphatidylcholine membranes: a comparative force field study. *J. Chem. Theory. Comput.* **2012**, *8*, 4593−4609.
(62) Gibbs, N.; Sessions, R. B.; Williams, P. B.; Dempsey, C. E. Helix bending in alamethicin: molecular dynamics simulations and amide hydrogen exchange in methanol. *Biophys. J.* **1997**, *72*, 2490−2495.
(63) Subbiah, R. N.; Kondo, M.; Campbell, T. J.; Vandenberg, J. I. Tryptophan scanning mutagenesis of the hERG K^+ channel: the S4 domain is loosely packed and likely to be lipid exposed. *J. Physiol.* **2005**, *569*, 367−379.
(64) Zhang, M.; Liu, J.; Tseng, G.-N. Gating charges in the activation and inactivation processes of the hERG channel. *J. Gen. Physiol.* **2004**, *124*, 703−718.
(65) Gong, Q.; Keeney, D. R.; Molinari, M.; Zhou, Z. F. Degradation of trafficking-defective long QT syndrome type II mutant channels by the ubiquitin-proteasome pathway. *J. Biol. Chem.* **2005**, *280*, 19419−19425.
(66) Satler, C. A.; Vesely, M. R.; Duggal, P.; Ginsburg, G. S.; Beggs, A. H. Multiple different missense mutations in the pore region of hERG in patients with long QT syndrome. *Hum. Genet.* **1998**, *102*, 265−272.
(67) Piper, D. R.; Hinz, W. A.; Tallurri, C. K.; Sanguinetti, M. C.; Tristani-Firouzi, M. Regional specificity of human ether-a′-go-go-related gene channel activation and inactivation gating. *J. Biol. Chem.* **2005**, *280*, 7206−7217.
(68) Ohgushi, M.; Wada, A. Molten-globule state - a compact form of globular proteins with mobile side chains. *FEBS Lett.* **1983**, *164*, 21−24.
(69) Soler-Llavina, G. J.; Chang, T. H.; Swartz, K. J. Functional interactions at the interface between voltage-sensing and pore domains in the Shaker K(v) channel. *Neuron* **2006**, *52*, 623−634.
(70) Es-Salah-Lamoureux, Z.; Fougere, R.; Xiong, P. Y.; Robertson, G. A.; Fedida, D. Fluorescence-tracking of activation gating in human ERG channels reveals rapid S4 movement and slow pore opening. *PLoS One* **2010**, *5*, e10876.
(71) Wang, Z.; Dou, Y.; Goodchild, S.; Es-Salah-Lamoureux, Z.; Fedida, D. Components of gating charge movement and S4 voltage-sensor exposure during activation of hERG channels. *J. Gen. Physiol.* **2013**, *141*, 431−443.
(72) Kanevsky, M.; Aldrich, R. W. Determinants of voltage-dependent gating and open-state stability in the S5 segment of Shaker potassium channels. *J. Gen. Physiol.* **1999**, *114*, 215−242.

(73) Upadhyay, S. K.; Nagarajan, P.; Mathew, M. K. Potassium channel opening: a subtle two-step. *J. Physiol.* **2009**, *587*, 3851−3868.
(74) Gustina, A. S.; Trudeau, M. C. HERG potassium channel regulation by the N-terminal eag domain. *Cell Signal* **2012**, *24*, 1592−1598.